ECCM '99

European Conference on
Computational Mechanics

August 31 – September 3
München, Germany

Computational Aspects of Nonlocal Models

Milan Jirásek

Laboratory of Structural and Continuum Mechanics (LSC)
Department of Civil Engineering (DGC)
Swiss Federal Institute of Technology at Lausanne (EPFL)
1015 Lausanne, Switzerland
e–mail: Milan.Jirasek@epfl.ch

Key words: Damage, Fracture, Localization, Nonlocal models, Consistent stiffness, Discontinuities

---

Abstract. *This paper deals with several issues related to computational analysis of strain localization problems using nonlocal continuum models of the integral type. Stress oscillations appearing for low-order elements are described, their source is detected, and possible remedies are proposed. The exact "nonlocal" tangential stiffness matrix is derived and its properties and the corresponding assembly procedure are discussed. Spurious shifting of the localization zone at late stages of the stiffness degradation process is described, and it is remedied by combining the nonlocal continuum description with explicitly modeled displacement discontinuities embedded in finite elements.*

---

1 Introduction

In the context of standard continuum theories, strain-softening constitutive models typically lead to ill-posed boundary value problems. Finite element solutions of such problems exhibit a pathological sensitivity to the element size and do not converge to physically meaningful solutions as the mesh is refined. The remedy is often sought in an enrichment of the classical continuum by nonlocal interaction, higher-order gradient effects, rate-dependent terms, or generalized stresses and strains (in the spirit of the Cosserat theory). Such enrichments enforce a certain minimal width of the zone of localized strains, and therefore they are called localization limiters.

A class of powerful localization limiters can be constructed by incorporating nonlocal effects into the constitutive equations. An overview of various nonlocal damage formulations and their evaluation have been presented in [1]. The present contribution shall focus on numerical aspects of such models. As their representative examples we consider the nonlocal damage model of Pijaudier-Cabot and Bažant [2] and the nonlocal rotating crack model with transition to scalar damage [3].

2 Nonlocal damage model

The simple isotropic damage model postulates the stress-strain law in the form

$$\boldsymbol{\sigma} = (1-\omega)\boldsymbol{D}^e\boldsymbol{\varepsilon} \tag{1}$$

where $\boldsymbol{\sigma}$ is the stress, $\boldsymbol{\varepsilon}$ is the strain, $\boldsymbol{D}^e$ is the elastic material stiffness matrix, and ω is a scalar damage parameter. For the specific version considered here, evolution of the damage parameter is controled by the damage energy release rate

$$Y = \frac{1}{2}\boldsymbol{\varepsilon}^T\boldsymbol{D}_e\boldsymbol{\varepsilon} \tag{2}$$

Initially, the damage parameter is equal to zero, and the response of the material is linear elastic. When the stored elastic energy reaches a certain critical value, the damage parameter starts growing, which reflects the gradual loss of integrity of the material. During unloading, characterized by a decreasing value of Y, the damage parameter remains constant. This can be taken into account by making ω dependent on the maximum previously reached value of Y, denoted as κ. The damage evolution is thus described by the explicit relation

$$\omega = f(\kappa) \tag{3}$$

and function f can be identified from the uniaxial stress-strain curve. Here we take a simple exponential softening law corresponding to Fig. 1.

In the nonlocal version of the model, the "local" damage energy release rate, Y, is replaced by its weighted average over a certain neighborhood of the given point,

$$\overline{Y}(\boldsymbol{x}) = \int_V \alpha(\boldsymbol{x},\boldsymbol{\xi})Y(\boldsymbol{\xi})\,\mathrm{d}\boldsymbol{\xi} \tag{4}$$

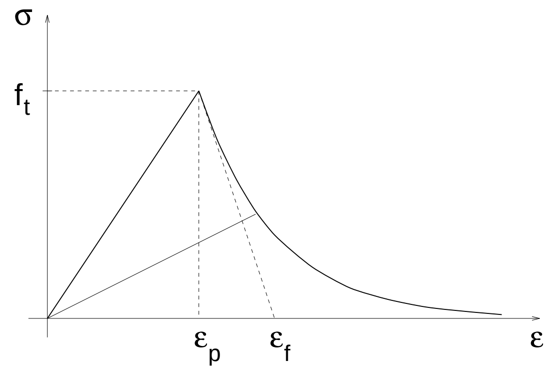

Figure 1: Stress-strain diagram with exponential softening

where $\alpha(\boldsymbol{x}, \boldsymbol{\xi})$ is a given *nonlocal weight function*. In an infinite specimen, the weight function depends only on the distance $r = ||\boldsymbol{x} - \boldsymbol{\xi}||$ between the "source" point, $\boldsymbol{\xi}$, and the "effect" point, $\boldsymbol{x}$. In the vicinity of a boundary, the weight function is usually rescaled such that the nonlocal operator does not alter a uniform field. This can be achieved by setting

$$\alpha(\boldsymbol{x}, \boldsymbol{\xi}) = \frac{\alpha_0(||\boldsymbol{x} - \boldsymbol{\xi}||)}{\int_V \alpha_0(||\boldsymbol{x} - \boldsymbol{\zeta}||)\,\mathrm{d}\boldsymbol{\zeta}} \tag{5}$$

where $\alpha_0(r)$ is a monotonically decreasing nonnegative function. It is often taken as the Gauss distribution function or as the bell-shaped function

$$\alpha_0(r) = \begin{cases} \left(1 - \dfrac{r^2}{R^2}\right)^2 & \text{if } 0 \le r \le R \\ 0 & \text{if } R \le r \end{cases} \tag{6}$$

where R is a parameter related to the internal length of the material (given by the size and spacing of major inhomogeneities). As R corresponds to the maximum distance of point $\boldsymbol{\xi}$ that affects the nonlocal average at point $\boldsymbol{x}$ we suggest to call it the *interaction radius.*

3 Stress oscillations

The first issue to be addressed is the appearance of stress oscillation patterns for certain types of meshes. For example, for a mesh composed of equilateral constant-strain triangles under uniaxial tension, elements in a layer perpendicular to the applied stress are at the same strain level but at two alternating stress levels. This is caused by the fact that the element centers, serving as integration points, do not have the same distance from the center of the localization zone. At points closer to the center of that zone, nonlocal strains are larger. Consequently, these points are more damaged and carry smaller stresses than integration points farther away from the localization zone. This phenomenon can be best documented by stress oscillations arising in linear one-dimensional elements if a higher-order integration scheme is used. Fig. 2 shows the (local) strain and stress profiles at several stages of the loading process for a bar under uniaxial tension, simulated with 20 linear finite elements and five integration points per element.

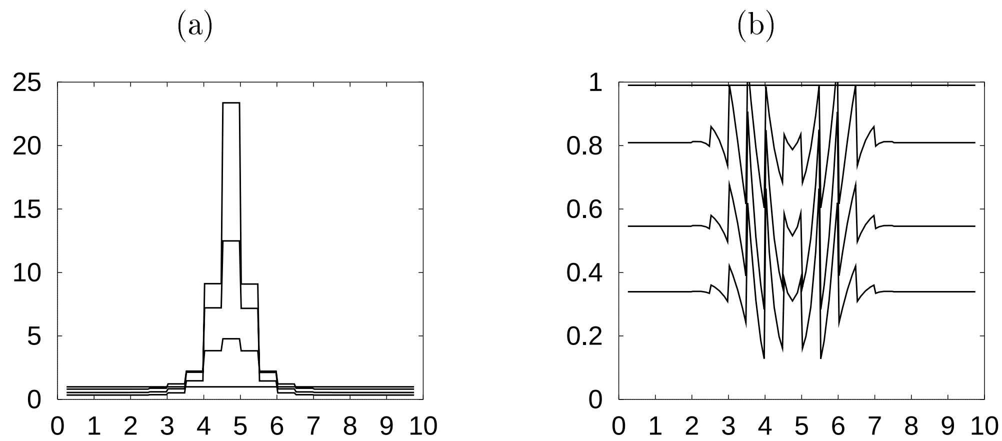

Figure 2: Profiles of a) local strain and b) stress

The source of the stress oscillations is in the unbalanced quality of approximation of local and nonlocal strains. Local strains are piecewise constant, with jumps at the interelement boundaries, while nonlocal strains obtained by weighted averaging of local ones are continuous. It is therefore natural to expect an improvement for higher-order elements. As demonstrated in [4], smooth shape functions constructed by the technique of moving least-squares approximations substantially reduce the stress oscillations. Alternatively, it is possible to construct a continuous strain interpolation by smoothing of the standard finite element interpolation. This technique is relatively simple and does not increase the number of degrees of freedom nor the number of integration points. It shall be described at the conference.

4 Consistent stiffness matrix for nonlocal models

Another interesting aspect of nonlocal models is the derivation of an exact tangential stiffness. Let us start from the standard formula for the vector of internal forces,

$$\boldsymbol{f} = \int_V \boldsymbol{B}^T(\boldsymbol{x})\boldsymbol{\sigma}(\boldsymbol{x})\,\mathrm{d}\boldsymbol{x} \tag{7}$$

where $\boldsymbol{B}$ is the strain-displacement matrix. In practice, the integral is replaced by a sum of contributions from a finite number of integration points $\boldsymbol{x}_p$,

$$\boldsymbol{f} = \sum_p w_p \boldsymbol{B}^T(\boldsymbol{x}_p)\boldsymbol{\sigma}(\boldsymbol{x}_p) \tag{8}$$

where w_p are integration weights and the summation index p is running from 1 to the total number of integration points. The nonlocal averaging integral in (4), defining the damage energy release rate at a given integration point, is also approximated by a finite sum,

$$\overline{Y}(\boldsymbol{x}_p) = \sum_q \alpha_{pq} Y(\boldsymbol{x}_q) \tag{9}$$

where α_{pq} are interaction coefficients that depend on the weight function α and on the volume represented by integration points $\boldsymbol{x}_q$.

Using the stress-strain law (1) and the standard strain approximation $\boldsymbol{\varepsilon}(\boldsymbol{x}) = \boldsymbol{B}(\boldsymbol{x})\boldsymbol{d}$ in which $\boldsymbol{d}$ is the vector of nodal displacements (or more general degrees of freedom), and introducing shorthand notation $\omega(\boldsymbol{x}_p) \equiv \omega_p$, $\boldsymbol{B}(\boldsymbol{x}_p) \equiv \boldsymbol{B}_p$, etc., we can expand (8) as

$$\boldsymbol{f} = \sum_p w_p(1-\omega_p)\boldsymbol{B}_p^T \boldsymbol{D}_p^e \boldsymbol{B}_p \boldsymbol{d} = \sum_p w_p(1-\omega_p)\boldsymbol{K}_p^e \boldsymbol{d} \tag{10}$$

where $\boldsymbol{K}_p^e = \boldsymbol{B}_p^T \boldsymbol{D}_p^e \boldsymbol{B}_p$. In the elastic range, $\omega_p = 0$ at all integration points, and (10) reduces to $\boldsymbol{f} = \boldsymbol{K}^e \boldsymbol{d}$ where $\boldsymbol{K}^e = \sum_p w_p \boldsymbol{K}_p^e$ is the elastic stiffness matrix.

The tangent stiffness matrix is obtained by differentiating the internal forces with respect to the nodal displacements. Note that the damage parameter in general depends on the nodal displacements (through interpolated strains that determine the damage energy release rates). To facilitate the differentiation, we precompute the derivative of the damage parameter at an arbitrary integration point with respect to the displacement vector, $\partial\omega_p/\partial\boldsymbol{d}$. If $\overline{Y}_p < \kappa_p$, the material state is inside the current elastic domain, and damage remains constant. In the opposite case, differentiation of the damage law (3) leads to

$$\frac{\partial\omega_p}{\partial\boldsymbol{d}} = f'(\overline{Y}_p)\frac{\partial\overline{Y}_p}{\partial\boldsymbol{d}} = f'(\overline{Y}_p)\sum_q \alpha_{pq}\frac{\partial Y_q}{\partial\boldsymbol{d}} \tag{11}$$

The finite element approximation of the (local) damage energy release rate at integration point q is

$$Y_q = \frac{1}{2}\boldsymbol{\varepsilon}^T \boldsymbol{D}_q^e \boldsymbol{\varepsilon} = \frac{1}{2}\boldsymbol{d}^T \boldsymbol{B}_q^T \boldsymbol{D}_q^e \boldsymbol{B}_q \boldsymbol{d} = \frac{1}{2}\boldsymbol{d}^T \boldsymbol{K}_q^e \boldsymbol{d} \tag{12}$$

and so

$$\frac{\partial Y_q}{\partial\boldsymbol{d}} = \boldsymbol{K}_q^e \boldsymbol{d} \tag{13}$$

Substituting this into (11) we obtain

$$\frac{\partial\omega_p}{\partial\boldsymbol{d}} = f'(\overline{Y}_p)\sum_q \alpha_{pq}\boldsymbol{K}_q^e \boldsymbol{d} \tag{14}$$

Now we can differentiate (10) and compute the tangent stiffness matrix

$$\boldsymbol{K} = \frac{\partial\boldsymbol{f}}{\partial\boldsymbol{d}} = \sum_p w_p(1-\omega_p)\boldsymbol{K}_p^e - \sum_p w_p \boldsymbol{K}_p^e \boldsymbol{d}\left(\frac{\partial\omega_p}{\partial\boldsymbol{d}}\right)^T = \tag{15}$$

$$= \sum_p w_p(1-\omega_p)\boldsymbol{K}_p^e - \sum_{p,q} w_p f'_p \alpha_{pq} \boldsymbol{K}_p^e \boldsymbol{d}\boldsymbol{d}^T \boldsymbol{K}_q^e \tag{16}$$

In this formula, f'_p has to be understood as $f'(\overline{Y}_p)$ in the case of loading and zero in the case of unloading/reloading below the current damage threshold. The first term,

$$\boldsymbol{K}^u = \sum_p w_p(1-\omega_p)\boldsymbol{K}^e_p \tag{17}$$

represents the secant stiffness matrix valid for unloading at all material points. Introducing a vector $\boldsymbol{f}^e_p = \boldsymbol{K}^e_p\boldsymbol{d}$, we can rewrite (16) in the final elegant form

$$\boldsymbol{K} = \boldsymbol{K}^u - \sum_{p,q} w_p f'_p \alpha_{pq} \boldsymbol{f}^e_p (\boldsymbol{f}^e_q)^T \tag{18}$$

The sum in (18) is a correction of the secant stiffness due to additional damage growth. In the local case, the interaction weights α_{pq} are given by Kronecker delta, and the sum can be performed over one subscript. In the nonlocal case, the individual terms $w_p f'_p \alpha_{pq} \boldsymbol{f}^e_p (\boldsymbol{f}^e_q)^T$ represent the contribution of nonlocal interaction between points $\boldsymbol{x}_p$ and $\boldsymbol{x}_q$ to the overall stiffness. Of course, the sum is performed only over those pairs of integration points that are closer than the interaction radius R (for other pairs the weight α_{pq} is zero). Each of these pairs contributes only to the block of the global stiffness matrix with rows corresponding to internal forces at the element containing point $\boldsymbol{x}_p$ and columns corresponding to nodal displacements at the element containing point $\boldsymbol{x}_q$. This means that the complete stiffness matrix can be assembled from much smaller matrices, similar to the usual assembly procedure. The difference is that the bandwidth increases due to the nonlocal interaction, and that the global stiffness matrix is in general not symmetric. The loss of symmetry is due to the nonsymmetric character of interaction weights α_{pq}.

The fully consistent tangential stiffness matrix can be exploited in the global equilibrium iteration procedure. The conference presentation shall provide examples illustrating the resulting acceleration of the convergence rate.

5 Combination with embedded discontinuities

Most nonlocal damage formulations, including those from [2] and 3], lead to a progressive shrinking of the zone in which local strains increase. For quasibrittle materials, this process naturally corresponds to the formation of a macroscopic crack. However, the thickness of the zone of increasing damage can never be smaller that the support diameter of the nonlocal weight function. When the residual stiffness of the material inside this zone becomes too small, numerical problems occur. This could be handled by removing the nodes connected to (almost) completely damaged elements from the mesh. However, in the presence of body forces the problem is more severe, because the center of the localization zone starts shifting even before the material is completely damaged. This is the case, e.g., in the analysis of gravity dams, where the effect of gravity forces is essential and cannot be neglected. The presence of gravity forces inside the fracture process zone leads to spurious shifting of the center of the zone and finally to the divergence of the equilibrium iteration process. This is documented in Fig. 3. A gravity dam with dimensions corresponding to

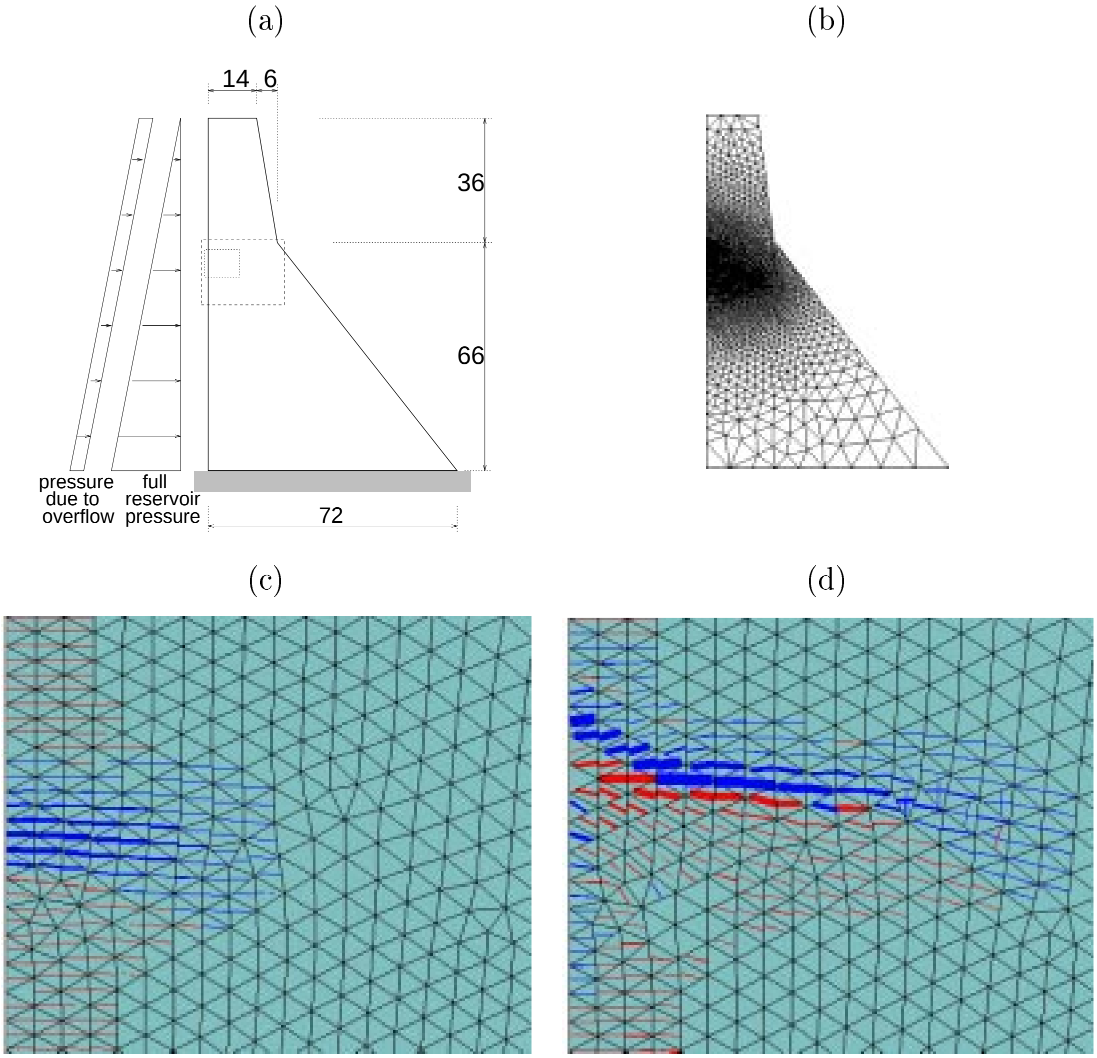

Figure 3: Analysis of a gravity dam: (a) Geometry and loading, (b) finite element mesh, (c-d) evolution of the crack pattern (close-up area is marked in (a) by a dotted rectangle)

the well-known Koyna Dam is loaded by its own weight, full reservoir pressure, and an increasing hydrostatic pressure due to reservoir overflow (Fig. 3a). The computational mesh, consisting of 4295 linear triangular elements, is shown in Fig. 3b. In a simulation using the nonlocal rotating crack model with transition to scalar damage [3], the initially diffuse cracking zone at the upstream face eventually localizes and propagates into the interior of the dam (Fig. 3c). Blue and red rectangles represent opening and closing smeared cracks, resp. When a critical degradation level is reached at the mouth of the macroscopic crack, the (constant) body forces start pulling the material down, which results into a shifting of the numerical crack (Fig. 3d) and later into the loss of convergence.

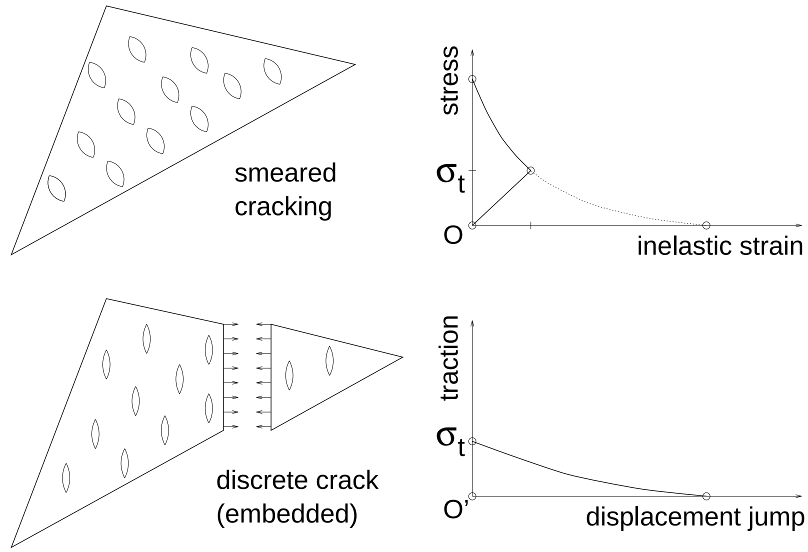

Figure 4: Transition from a continuum model to a discontinuity

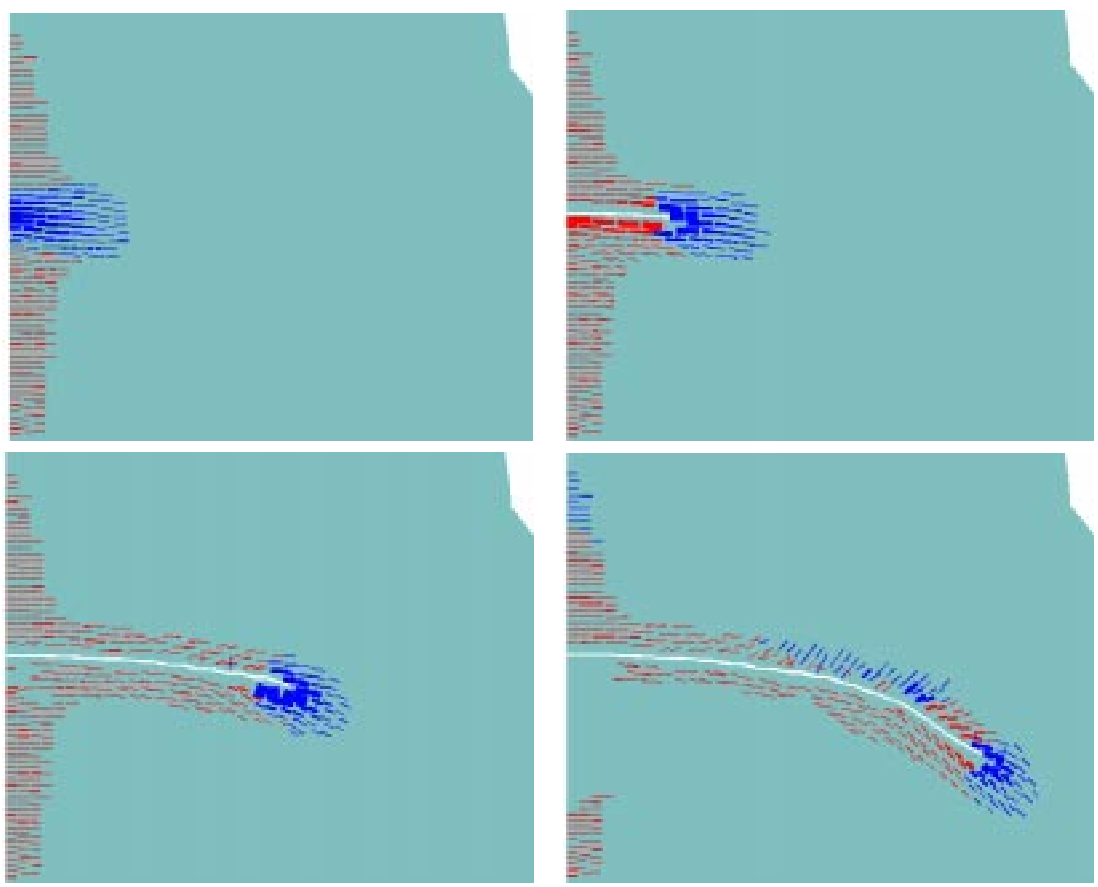

Figure 5: Fracture process zone development and propagation of a discrete crack modeled as a displacement discontinuity embedded in finite elements (close-up area is marked in Fig. 3a by a dashed rectangle)

An elegant remedy can be based on the transition from highly localized strains to displacement discontinuities embedded in the interior of finite elements [5]. Such an approach is appealing from the physical point of view, because in the final stage of the degradation process the material should no longer be considered as a continuum. As fracture progresses, long-range interaction between material points becomes more difficult and finally impossible. This would be best reflected by a nonlocal model with an evolving (decreasing) characteristic length. However, such a model would be computationally very expensive, since the interaction weights for all interacting pairs of integration points would have to be continuously recomputed. The approach proposed in [5] can be considered as a reasonable approximation, with a constant interaction length in the early stage of degradation and a zero interaction length in the final stage.

The simulation of the gravity dam has been repeated using the model with transition from nonlocal rotating cracks to embedded displacement discontinuities (discrete cracks) [5]. The transition takes place when the cracking strain reaches a certain critical value, and the softening laws describing the smeared and discrete parts of the model are matched such that a smooth transition and correct energy dissipation are ensured; see Fig. 4. The initial cracking pattern is the same as before, but soon after localization the first discrete crack appears and propagates along the center of the fracture process zone (see the white lines in Fig. 5). The partially damaged material in the wake of the discrete crack unloads, and its residual strength does not diminish anymore. Therefore, the correct crack trajectory can be captured without any numerical instabilities.

6 Comparison to gradient models

Finally, let us add a few general comments comparing nonlocal integral models to models that incorporate nonstandard gradient terms into the constitutive equations [6-8]. The basic version of the integral formulation seems to be easier to implement and its behavior is relatively robust. No additional degrees of freedom are needed, and only equilibrium equations have to be solved on the global level. On the other hand, the tangential stiffness matrix has a larger bandwidth, and nonlocal averaging increases the need for data exchange between neighboring subdomains, which complicates the parallelization of the code and reduces its efficiency. Also, gradient models seem to be more flexible if the characteristic length evolves during the degradation process, or if the averaging operator gradually acquires certain anisotropic properties. The physical meaning of nonstandard boundary conditions required by gradient models is often questioned, but it should be admitted that for nonlocal integral models an analogous problem arises—the modification of the averaging operator in the proximity of a boundary is also intuitive and somewhat ambiguous. This means that both classes of localization limiters have their advantages and drawbacks, and the choice of the optimal approach depends on the exact nature of the underlying constitutive model.

7 Conclusions

Stress oscillations arising in finite element simulations with nonlocal models have been described and their source has been detected. The possible remedies are still under investigation and shall be discussed in more detail in the conference presentation.

The exact, fully consistent global stiffness matrix has been derived for the nonlocal isotropic damage model with damage energy release rate as the variable driving the growth of damage. Due to the long-distance interaction, the stiffness matrix has a larger bandwidth than for a local model and is in general nonsymmetric. Nonstandard contributions must be taken into account during the assembly procedure. Nevertheless, a fully consistent tangential stiffness matrix can be constructed and exploited in the global equilibrium iteration procedure.

Spurious shifting of the fracture process zone due to gravity forces has been described and it has been demonstrated that the transition from nonlocal continuum to a directly modeled displacement discontinuity embedded in finite elements can remedy the problem.

References

[1] M. Jirásek. *Nonlocal models for damage and fracture: Comparison of approaches.* International Journal of Solids and Structures, **35**, 4133–4145, (1998).

[2] G. Pijaudier-Cabot and Z. Bažant. *Nonlocal damage theory.* Journal of Engineering Mechanics ASCE, **113**, 1512–1533, (1987).

[3] M. Jirásek and T. Zimmermann. *Rotating crack model with transition to scalar damage.* Journal of Engineering Mechanics ASCE, **124** (3), 277–284, (1998).

[4] M. Jirásek. *Element-free Galerkin method applied to strain-softening materials.* In: R. de Borst, N. Bićanić, H. Mang, and G. Meschke (eds.), Computational Modelling of Concrete Structures, Balkema, Rotterdam (1998), 311–319

[5] M. Jirásek. *Embedded crack models for concrete fracture.* In: R. de Borst, N. Bićanić, H. Mang, and G. Meschke (eds.), Computational Modelling of Concrete Structures, Balkema, Rotterdam (1998), 291–300

[6] I. Vardoulakis and E.C. Aifantis. *A gradient flow theory of plasticity for granular materials.* Acta Mechanica, **87**, 197–217, (1991).

[7] H.-B. Mühlhaus and E.C. Aifantis. *A variational principle for gradient plasticity.* International Journal of Solids and Structures, **28**, 845–857, (1991).

[8] R.H.J. Peerlings, R. de Borst, W.A.M. Brekelmans and J.H.P¿ de Vree. *Gradient enhanced damage for quasi-brittle materials.* International Journal for Numerical Methods in Engineering, **39**, 3391–3403, (1996).